Chapter 3

Photocatalytic Activity of TiO_2 Nanostructured Arrays Prepared by Microwave-Assisted Solvothermal Method

Ana Pimentel, Daniela Nunes, Sónia Pereira,
Rodrigo Martins and Elvira Fortunato

Additional information is available at the end of the chapter

http://dx.doi.org/10.5772/63237

Abstract

The use of metal-oxide-semiconductor nanostructures as photocatalytic materials has been an area of intense research over the last decade, and in this field, titanium dioxide (TiO_2) receives much attention. TiO_2 is an attractive material since it is stable, insoluble, non-toxic, resistant to corrosion and relatively inexpensive. In this chapter, we will demonstrate the influence of different solvents on the synthesis of TiO_2 nanostructures considering a solvothermal method assisted by microwave radiation and their photocatalytic behaviour. The TiO_2 nanostructured arrays were synthesized on seeded polyethylene naphthalate (PEN) substrates with different solvents: water, 2 – propanol, ethanol and methanol. TiO_2 thin films deposited by spin-coating were used as seed layer for the nanostructures growth. Structural characterization of the microwave synthesized materials has been carried out by scanning electron microscopy (SEM) and X-Ray diffraction (XRD). The optical properties have also been investigated. The TiO_2 nanostructures arrays were tested as photocatalytic agents in the degradation of pollutant dyes like methylene blue (MB) in the presence of UV radiation. Expressive differences between the different solvents were detected, in which methanol demonstrated higher MB degradation for the conditions tested.

Keywords: titanium dioxide, nanostructures, microwave radiation, solvents, photocatalysis

1. Introduction

Titanium dioxide (TiO_2) is a n-type semiconductor material that has attracted considerable attention in several applications, such as sensor devices [1], dye-solar cells [2], photocatalysis

[3], among others. Lately, the growing interest in this material is mainly associated to its long-term photostability, non-toxicity, low cost availability [4] and for being a semiconductor material, with a band gap of approximately 3 eV. Moreover, this material is sensitive to UV radiation, with notable transmittance in the visible region (superior to 80%), high refractive index (between 2.5 and 2.7) and chemical stability [5].

1.1. TiO_2 as a photocatalyst material

Titanium dioxide is non-toxic, chemically stable, earth-abundant and inexpensive, being considered attractive as a photocatalytic material [6]. TiO_2 photocatalytic activity is directly related to size, specific surface area, impurities on crystalline phase, and the exposed surface facets [7], thus several TiO_2 nano/micro structures were reported in order to improve its final performance [7].

One-dimensional nanostructures, such as nanowires and nanorods, offer a higher surface to volume ratio, when compared to other type of morphologies, which turn them interesting to photocatalytic application. Nevertheless, when these nanostructures are used in the powder form, the separation of the catalyst from solution becomes a problem, which makes the use of films highly appealing. Moreover, when included the option of using flexible substrates, such as polyethylene naphthalate (PEN) on these nanostructured films, opens to a broad range of possibilities and low cost strategies.

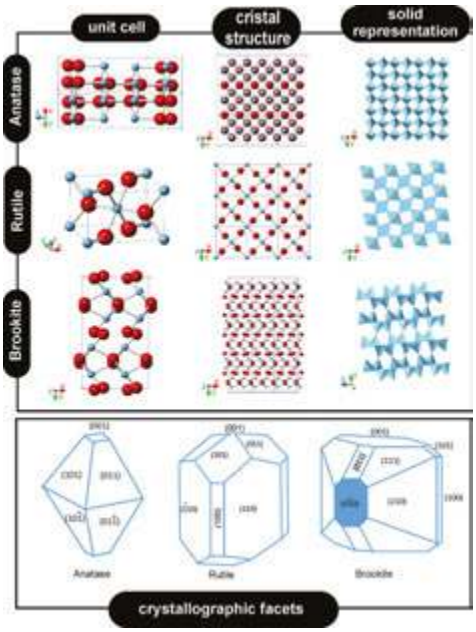

Figure 1. Crystallographic structures of different TiO_2 crystals: anatase, rutile and brookite.

http://dx.doi.org/10.5772/63237

TiO_2 used as a photocatalytic material for decomposition of organic pollutants and its photocatalytic activity has been reported in several different studies [3, 8, 9]. Rutile and anatase structures are the most important phases for TiO_2. TiO_2 can exist in amorphous form or in three crystalline phases: rutile (a tetragonal structure, $P4_{2/mmm}$), anatase (also a tetragonal structure, $I4_{1/amd}$) and brookite (an orthorhombic structure, Pbca), at ambient temperature [10], as shown on **Figure 1**. Among these three different phases, rutile is the one with the most stable phase. The optical band gap of titanium dioxide is slightly above 3 eV (rutile: 3.0 eV, anatase: 3.4 eV and brookite: 3.3 eV) [10].

TiO_2 in the form of anatase is the most used as a photocatalyst under UV radiation [11]. Rutile has a smaller electron effective mass, higher density and higher refractive index [5]. Anatase contains more defects in the lattice, producing more oxygen vacancies and capturing the electrons [12]. Moreover, the later possesses a shallow donor level, high electron mobility and trap controlled electronic conduction [13]. Considering such properties, the anatase form is preferred to be used in most optoelectronic and photocatalyst applications. Anatase and rutile are generally regarded to be used in photocatalytic applications, while brookite is not.

An n-type semiconductor has a filled valence band (VB) and an empty conduction band (CB). The absorption of a photon (with an energy at least equal to the bandgap) by TiO_2 nanoparticles will result in the promotion of an electron, e^-, from the valence band to the conduction band, leaving behind a "hole", h^+, (an electron vacancy) in the VB [14]. For anatase and rutile, as mentioned above, the bandgaps values are 3.2 and 3.0 eV (corresponding to wavelengths of 385 and 410 nm), respectively. Ultraviolet light is necessary for the material photoexcitation. The electron-hole pairs can recombine or participate in chemical reactions with the surface adsorbed species.

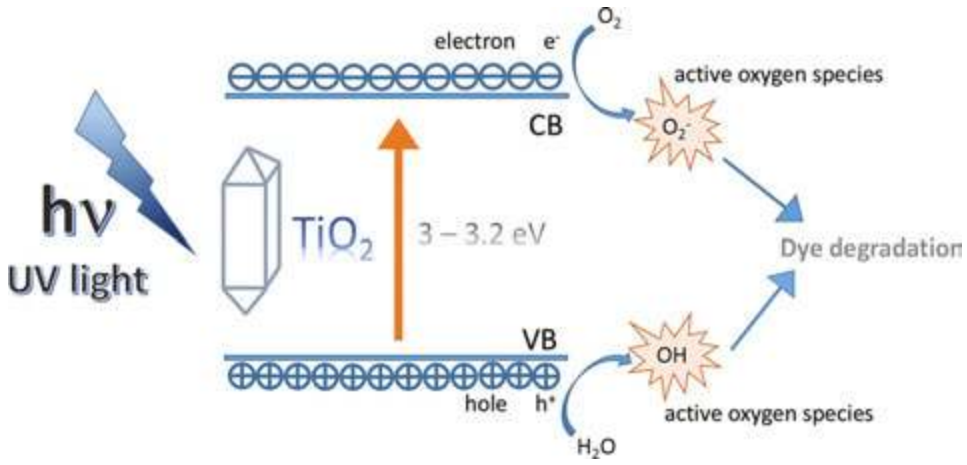

Figure 2. Schematic of the titanium dioxide band levels in the presence of UV radiation.

The electron-hole, h^+, in the valence band provides a site where the adsorbed hydroxyl ions (OH^-) and disassociated water (H_2O) can lose an electron forming a hydroxyl radical ($OH\cdot$). Hydroxyl radicals are electrically neutral but highly reactive. The CB electrons (e^-) can react with molecular oxygen (O_2) and form the superoxide radical-anion, O_2^-, which will also be involved in reaction of dye degradation [15]. In addition, the hole h^+ and the electron e^- can react directly with adsorbed pollutants (see **Figure 2**).The excitation of valence band electrons to the conduction band allowing for the formation of hydroxyl radicals is what makes TiO_2 a catalyst.

The catalysts materials at the nanoscale have the advantage of presenting large surface area and, therefore, larger number of active sites per volume to promote the photocatalytic reaction. Smaller particle sizes imply shorter distances for photogenerated charge carriers to migrate before reaching surface reaction sites [16].

As photocatalytic redox reactions take place on the crystal surface, the surface reactivity of TiO_2 strongly influences the material photocatalytic activity [17]. The effect of particle shape on the photochemistry also plays an important role. It has been demonstrated that some crystal orientation are much more reactive than others, so the overall reactivity could be related to the particle shape [16].

The TiO_2 nanocrystal growth is based on the minimization of surface energy, which will lead to the disappearance of the most reactive facets [18]. In general surfaces with higher surface energy disappear rapidly during the crystal growth process in order to minimize the total surface energy.

The equilibrium shape of anatase crystal consists of a truncated tetragonal bipyramidal structure constructed by eight {101} facets and two top squared {001} facets [19] (see **Figure 1**). For rutile, the equilibrium shape consists of a tetragonal prism bounced by a {110} facet and terminated by two tetragonal pyramids bounded by {011} facets [20]. In the case of brookite, the equilibrium crystal possesses seven different facets [20]. The equilibrium shape of the latter materials will vary according to the growth conditions employed and the different facets will present different properties.

The photocatalytic oxidation and reduction sites of rutile were reported as being present on the {011} and {110} facets, respectively. In the case of anatase, it was mainly present in {001} and {011} facets, respectively [20, 21] (see **Figure 3**). Brookite has not attracted much attention for photocatalytic applications due to its lack of photocatalytic activity. In contrast to this latter, anatase has the {101} surface facet, for which only 50% of the Ti atoms are five-coordinated (Ti_{5c}), both the {001} and {100} surfaces facets consist of 100% Ti_{5c} atoms [17]. These atoms act as active sites in the photocatalytic experiments, so by this reason, the facets {001} and {100} should be more active than {101} facets.

The origin of the higher reactivity of these facets can be associated to the increased density of undercoordinated Ti atoms at the surface and to the surface atom arrangement [22].

http://dx.doi.org/10.5772/63237

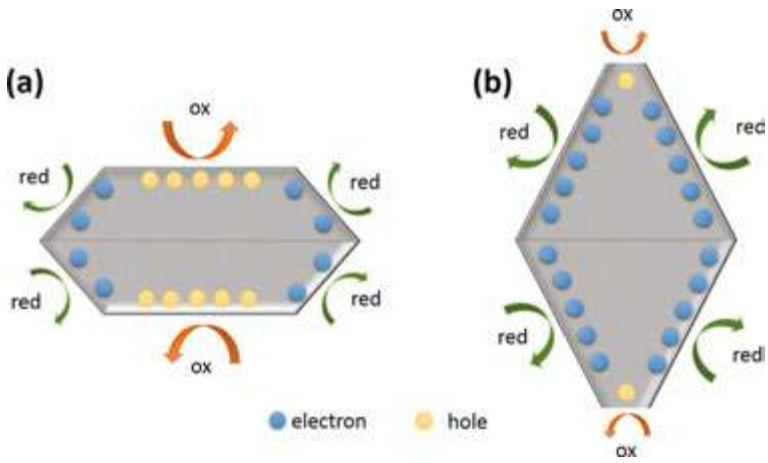

Figure 3. Schematic images of spatial separation of redox sites on titanium dioxide structures with a specific exposed crystal facets: (a) larger surface area of oxidation sites (holes) and small surface area of reduction sites (electrons), and (b) smaller surface area of oxidation sites and larger surface area of reduction sites.

1.2. Solvothermal method assisted by microwave radiation

The structural, optical and electrical properties of titanium dioxide nanostructures strongly depend on the growth method. Several chemical, electrochemical and physical techniques have been employed to grow different TiO_2 nanostructures [3, 23–26] with different properties, like thermal evaporation [27], potentiostatic anodization [28], electrospinning [29], precipitation [30], solvothermal and hydrothermal synthesis, whether by conventional heating [31] or microwave radiation [3]. The use of this latter synthesis technique has been growing lately for different types of nanostructured semiconductors [3, 32–36].

The greatest advantage of using microwave radiation synthesis is related to the opportunity to complete reactions in a short period of time, when compared with conventional heating. Microwave radiation transfers the energy directly to the reactive species of the solutions favoring some transformations that are unobtainable with conventional heating [37]. By coupling directly with the molecules dipoles, the microwaves promote a rapid increase of temperature, originating a localized superheating of the molecules, which thus influences the solution [37].

So, the heating with microwave process occurs by two distinct mechanisms: through dipole rotation and/or ionic conduction, by the reversals of dipoles and displacement of charged ions present in the solution (solute and solvent) [38].

The heating caused by dipole rotation movement is due to an energy transfer between molecules when their dipoles try to align with the electric field changing of the electromagnetic radiation (see **Figure 4**). The coupling efficiency of dipoles with the electric field is related with the solution molecules polarity [37].

The heating due to ionic conduction movement results from the free ions or ionic species movement present in the solution. The friction between this species results in the increase of solution temperature [37].

So, microwave heating is mainly characterized by energy transfer between molecules, while conventional heating is characterized by energy transfer through convection, thermal conduction or radiation between the vessels external materials to the solution. Microwave radiation will interact with the solution molecules, converting the electromagnetic energy into thermal energy [40].

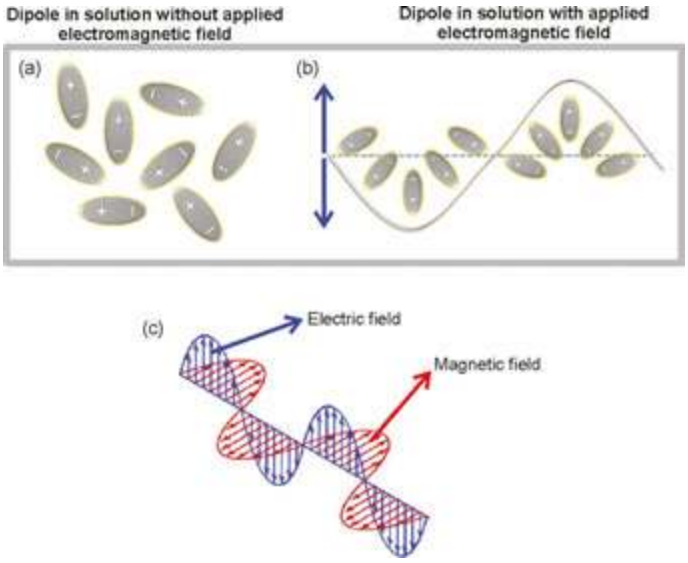

Figure 4. (a) Dipoles in the solution with no applied field; (b) dipoles alignment with the applied field; (c) Schematic representation of an applied electromagnetic field.

By this reason, it can be concluded that the use of different solvents will be relevant in organic synthesis. The polarity of a solvent is one of the most important parameters to be considered in microwave synthesis. The ability of a molecule to couple with microwave energy increases with the increase of solution polarity and thus the heating is more efficient.

The interaction between a polar molecule and microwave radiation can be estimated by the Loss Tangent (tan δ, see Equation 1), that determines the ability that a solvent possesses in absorbing microwave radiation and convert the electric energy into heat. This parameter give us the efficiency of microwave heating of a certain solvent [39, 41]:

$$\tan \delta = \frac{\varepsilon''}{\varepsilon'}$$

http://dx.doi.org/10.5772/63237

where ε″ is the loss factor that determines the efficiency of converting absorbed microwave energy into heat; ε′ is the dielectric constant that measure the ability of a molecule to store electrical potential energy with an applied electric field.

Thus, the higher the Loss Tangent (tan δ) is, the better will be the solvent in absorbing the microwave radiation and converting it into heat [37, 39].

Table 1 shows the loss tangents, dielectric constant, boiling point and viscosity of different types of solvents, including water, ethanol, 2 - propanol and methanol [37, 42, 43].

The solvents with higher values of dielectric loss are considered higher absorbers, which leads to the fast heating of the solution with the presence of microwave radiation. The solvents that are considered medium absorbers, also heat the solution efficiently but require more time to reach the synthesis temperature. The low absorbers solvents can heat to temperatures high above the solution boiling point, but longer times or higher microwave power is necessary.

	Solvent	*Tan δ*	*Dielectric Constant*	*Boiling point (°C)*	*Viscosity (cP) at 25 °C*
High	Ethylene glycol	1.17	38.0	197.3	35.7
(tan δ > 0.5)	**Ethanol**	**0.94**	**24.6**	**78.4**	**0.983**
	2 – propanol	**0.80**	**20.2**	**82.6**	**2.040**
	Methanol	**0.66**	**33.0**	**64.7**	**0.507**
	1 – butanol	0.57	17.8	117.6	2.573
Medium	2 – butanol	0.45	15.8	98.0	3.100
(0.1 < tan δ < 0.5)	Dichlorobenzene	0.28	9.9	180.5	1.320
	Acetic acid	0.17	6.1	118.0	1.060
	Dichloroethane	0.13	10.7	84.0	0.780
	Water	**0.12**	**80.0**	**100.0**	**0.890**
Low	Chloroform	0.091	4.8	61.2	0.510
(tan δ < 0.1)	Ethyl Acetate	0.059	6.0	77.0	0.420
	Acetone	0.054	21.0	56.0	0.300
	Toluene	0.040	2.4	111.0	0.560
	2 - ethoxyethanol	0.039	3.3	135.0	2.100

Table 1. Loss tangents, dielectric constant, boiling point and viscosity of solvents.

The viscosity of a solvent is also an important factor, as it will affect its ability to absorb microwave energy since it will affect the molecular rotation. In a high viscous medium, molecular mobility is reduced, thus making it difficult for the molecules to align with the electromagnetic radiation. By this reason, the heat produced by dipole rotation decreases [38].

As mentioned above, the use of different solvents could strongly affect the crystalline phase and microstructure of TiO_2 structures and its facets, due to the different boiling points, chain

lengths and structure, possible complexes and polarity of the solvents used [44–47]. For this case, the selection of the solvent should consider the high extracting power and strong interaction with electromagnetic field. Polar molecules and ionic solutions strongly absorb microwave energy due to the permanent dipole moment. Non-polar solvents will not heat up.

2. Methods used

2.1. Seed layer and synthesis of TiO_2 nanostructured arrays

The TiO_2 thin film to serve as a seed was deposited on a flexible PEN (Polyethylene naphthalate) substrate using the spin-coating method. A coating solution have been prepared from titanium isopropoxide ($Ti[OCH(CH_3)_2]_4$; 97%, CAS: 546-68-9), ethanolamine, MEA (C_2H_7NO; 99%, CAS: 141-43-5) and 2-methoxyethanol ($C_3H_8O_2$, 99.8%, CAS: 109-86-4), all from Sigma-Aldrich, that were used without further purification. In a typical experiment, the spin-coating solution was prepared by dissolving the $Ti[OCH(CH_3)_2]_4$ in 2-methoxyethanol and adding the ethanolamine. The concentration of the solution was chosen to be 0.35 M, in a proportion of 1:1 of titanium isopropoxide and ethanolamine. The resulting solution was then stirred for 2 hours at 60°C. The mixed solution was filtered to yield a clear and homogeneous solution and then used for preparing films by spin-coating method. Before deposition, the substrates (with 20 × 20 mm side) were successively cleaned with ethanol, and deionized water in an ultrasonic bath. The prepared solution was then spin coated on the substrate at 3000 rpm for 35 seconds at room temperature. After deposition, the films were dried at 180°C for 10 minutes in a hot plate in order to remove the solvent. After repeating the coating – drying cycles 4 times, the substrates were annealed for 1 hour at a temperature of 180°C.

After uniformly coating the PEN substrates with TiO_2 thin films, TiO_2 nanostructured arrays were synthesized by solvothermal method assisted by microwave radiation. The solution has been prepared from titanium isopropoxide ($Ti[OCH(CH_3)_2]_4$; 97%, CAS: 546-68-9), hydrochloric acid (HCl; 37% CAS: 7647-01-0) and as solvent it was used double distilled water, isopropyl alcohol (or 2 – propanol, $(CH_3)_2CHOH$, 99.5%, CAS: 67-63-0), ethanol (CH_3CH_2OH, 99.5%, CAS: 64-17-5) and methanol (CH_3OH, 99.8%, CAS: 67-56-1). In a typical reaction, 15 ml of HCl was added to 45 ml of each solvent. To each of these mixtures were added 2 ml of titanium isopropoxide. The solutions were stirred for 10 minutes.

The synthesis of TiO_2 nanostructures were performed by solvothermal method assisted by microwave radiation using a CEM Focused Microwave Synthesis System Discover SP. The TiO_2 seeded PEN substrates (20 × 20 mm) were placed at an angle against the vessel, with the seed layer facing down (see **Figure 5**) and filled with 20 ml of the prepared solution [3]. Time, power and maximum pressure (limited pressure) have been set at 120 min, 100 W and 250 Psi, respectively. The vessels were kept sealed by the constraining surrounding pressure. The temperature was kept at 110°C due to the use of flexible substrates.

http://dx.doi.org/10.5772/63237

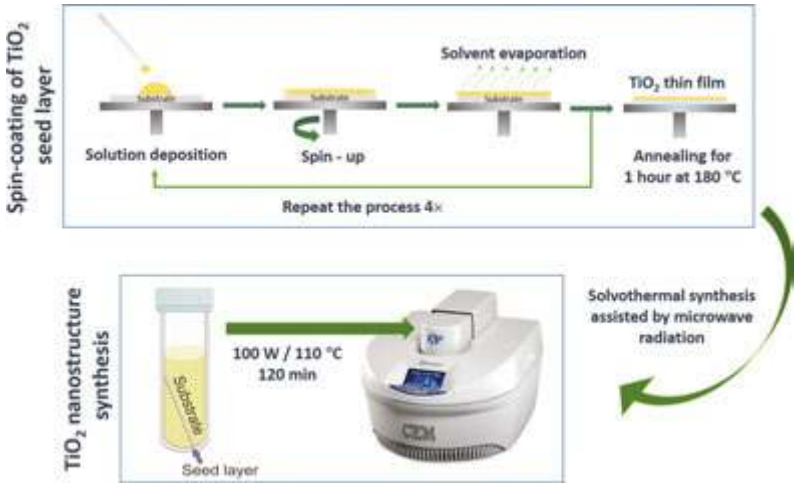

Figure 5. Scheme of the TiO_2 seed layer production using the spin-coating method, followed by TiO_2 nanostructured synthesis by solvothermal method assisted by microwave radiation.

2.2. Characterization techniques

The surface morphology and cross-section observations of TiO_2 nanocrystals has been characterized by scanning electron microscopy (SEM) with a Carl Zeiss AURIGA equipment coupled with an X-ray Energy Dispersive Spectrometer (EDS). X-ray diffraction measurements were carried out using a PANalytical's X'Pert PRO MRD, with a monochromatic Cu$K\alpha$ radiation source (wavelength 1.540598 Å) and from 30° to 75° (2θ), in a parallel beam configuration for grazing-incident experiments. The grazing XRD data were recorded with the detector rotated to a 0D configuration and at grazing-incident angles of 0.75, 1.0 and 1.25° with a step size of 0.1°. For comparison, rutile, anatase, brookite power diffractograms have been simulated with PowderCell [48] using crystallographic data from [49].

Optical transmittance and band gap measurements of the TiO_2 nanorods films were performed at room temperature (RT) using a Perkin Elmer lambda 950 UV/VIS/NIR spectrophotometer. The transmittance spectra were recorded between 250 to 850 nm.

2.3. Characterization of TiO_2 nanostructured arrays as photocatalytic agent

TiO_2 nanostructures arrays have been used in photocatalytic degradation of organic pollutants due to their non-toxic and higher photocatalytic efficiency with good sensing behaviour. The ultra violet (UV) photocatalytic activities of TiO_2 nanostructures were evaluated at RT from the degradation of methylene blue, MB, ($C_{16}H_{18}ClN_3S{\cdot}3H_2O$, CAS: 61-73-4) from Scharlau. The experiments were carried out following the International standard ISO 10678. The MB concentration used was 4 mg/l, in which a PEN substrate with the TiO_2 nanostructured array produced with each solvent was immersed in 50 ml of this solution for each experiment. Prior

to UV exposure, the sample was placed in the dark for 30 min to establish absorption-desorption equilibrium.

For UV exposure, a deuterium lamp model L11798 was used, from Hamamatsu, with an emission wavelength of 160 nm. In each measurement, 4 ml of MB solution were collected regular intervals (from 15 min up to a total time of 120 min). At each time, it was tested by a UV-Vis spectrophotometry, using the same Perkin Elmer lambda 950 UV/VIS/NIR spectrophotometer. The absorbance (A) was obtained between 250 to 800 nm.

3. Results and discussion

Figure 6 shows a real image of the materials produced after microwave radiation. As it can be seen, the substrates are fully covered demonstrating that the seed layer is efficient for the TiO_2 nanostructured arrays growth (the edges are seed/arrays free, due to the use of kapton tape for support). Moreover, this also demonstrates that microwave synthesis using flexible substrates is a valid option for low cost applications. Regarding the solvents tested, several solvents were used; however only the ones presented on this study resulted in a homogeneous growth of TiO_2 nanostructures covering completely the PEN substrate.

Figure 6. Photograph of TiO_2 nanostructured arrays on PEN substrates. All solvents produced similar samples, such as the one presented in this image.

3.1. Behaviour of solvents under microwave radiation

To infer the solvent behaviour under microwave radiation, the temperature and pressure profile of each solvent during TiO_2 synthesis was recorded and is presented on **Figure 7**. Pressure and temperature are two important parameters that will influence the nanoparticle morphology [50]. So, in a typical microwave assisted synthesis, in which the temperature is controlled, the path will involve ramping up to the desired temperature and holding the

http://dx.doi.org/10.5772/63237

desired temperature for a specific period of time, while the power fluctuates in order to maintain the parameters of the reaction (temperature and pressure). Once the holding time is complete, the reaction is quenched by a stream of nitrogen in order to cold down the vessel and the solution.

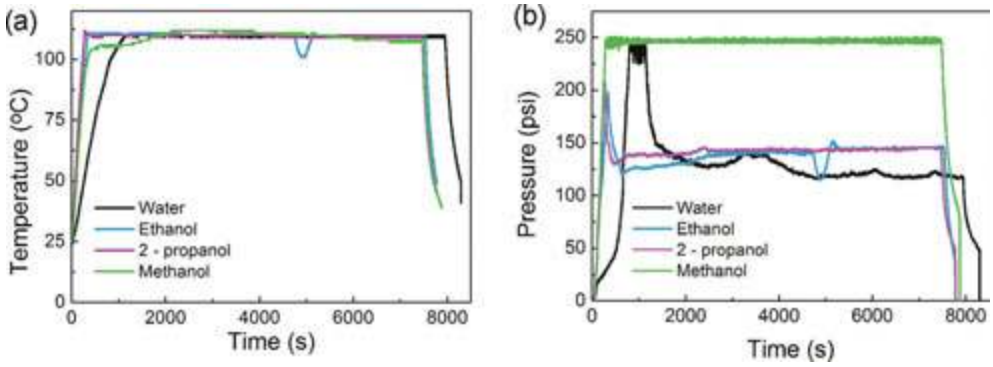

Figure 7. Profile of (a) temperature and (b) pressure obtained during TiO_2 nanostructured synthesis with different solvents, water, ethanol, 2 – propanol and methanol, when subject to microwave radiation of 100 W for 120 minutes and a pressure limit of 250 Psi.

As expected and in accordance to the values presented in **Table 1** (***Tan δ)***, in the case of water (a medium absorber), it took a longer period of time to reach the synthesis temperature when compared to the other solvents (all considered higher absorbers), see **Figure 7.a**).

The other parameter that is imperative to control in microwave assisted synthesis is the pressure inside the vessel. A pressurized environment can bring some advantages. As the temperature of a solvent increase above its boiling point, more pressure builds inside the reaction vessel [37]. From **Figure 7**, it is possible to observe that methanol (the solvent with a lower boiling point) originated a higher pressure value inside the reaction vessel.

3.2. SEM analysis

It is well known that for preparing uniform nanoparticles, it is necessary to induce a single nucleation event and thus preventing additional nucleation during the subsequent growth process [51]. Nevertheless, the presence of inorganic and organic anionic species in the starting solution will affect parameters such as nucleation, crystal growth and morphology of nanoparticles [52]. Moreover, synthesis employing different solvents, such as the ones used in this work, is highly expected to affect the crystalline phase, microstructure and optoelectronic properties of the produced nanoparticles, mainly due to the difference in the boiling point, chain lengths and structure, coordination numbers and polarity [5].

As it has been shown previously, the heating and pressure inside the reaction vessels will greatly depend on the solvents and precursors used. By this reason, it is clear that the temperature of reaction and the heating method will strongly influence the nucleation and crystal

growth, which will produce effect on size, shape, morphology and crystal structure (crystal facets) of the final synthesized nanoparticle.

Figure 8 shows the morphology of TiO_2 nanostructures formed with the different solvents under 100 W for 120 minutes with limited temperature and pressure of 110°C and 250 Psi, respectively. The microwave synthesis with water as solvent resulted in agglomerates with higher packing density of TiO_2 nanorods, forming compact structures (see **Figure 8.a**) and displaying average width of ~20 nm and length ranging from 1 to 1.5 μm. These results are in agreement to [3], where thin and long nanorods were observed using the same proportion of water/acid. Ethanol, on the other hand, resulted in TiO_2 nanorods with approximately 20 nm in width, however smaller in length (see **Figure 8.b**). The length varied from 800 to 1000 nm. When using 2 – propanol, the array structures varied and turned to be a mixture of nanorods and nanoparticles without a defined shape. These mixed nanostructures appeared as agglomerates of flower-like TiO_2 nanostructures (see **Figure 8.c**). The agglomerate sizes varied from 800 to 1100 nm. Methanol resulted in TiO_2 nanowires (~20 nm in width) grouped in agglomerates (see **Figure 8.d**). The compact structure observed with water was not observed, where the nanorods appeared to be well separated. Two sources of structures could be detected on the cross-section image, forming a dense layer of TiO_2 nanorods at the bottom with nanorod agglomerates on top. The total length of these structures together varied from 800 to 1000 nm. From the cross-section images, it could be identified that the arrays were grown with similar thickness, despite the disparities on the structures observed.

In solvothermal synthesis reactions, the temperature has been reported as one of the most important parameters to control the morphology of nanoparticles [52, 53]. In this present study, the synthesis temperature was limited to 110°C, due to the use of a low temperature polymeric substrate, so it will be the pressure inside the vessel that is going to play an important role in the TiO_2 nanostructure synthesis.

The use of water, with a higher boiling point but lower *tan δ*, and thus with a small microwave coupling efficiency [37], induces a lower heating rate and lower pressure inside the reaction vessel. The produced nanorods are longer in length (slower reaction rate induces large particle size). On the other hand, the nanorods produced with ethanol are smaller in length, and this can be associated to the fact that ethanol displays a higher value of *tan δ*, and a lower boiling point (when compared with water) and in consequence with higher microwave coupling efficiency and thus higher heating rate resulting in slightly higher pressure inside the vessel (faster reaction rate induces smaller particle size) [54].

In the case of 2 – propanol, as this solvent presents a medium value of *tan δ* (see **Table 1**) it is one of the most efficient in terms of coupling with microwave radiation. In this case, it is expected to be promoted a rapid growth of TiO_2 nanostructures. On the other hand, this is the solvent that presents higher value of viscosity which will reduce the dipole movement on the solution. The diffusion of ions in the solvent decrease with increasing viscosity [55].These characteristics are expected to be responsible for the undefined structures observed for this solvent.

http://dx.doi.org/10.5772/63237

Due to the very low boiling point of methanol, the pressure inside the reaction vessel increases rapidly, reaching the imposed limit. The synthesis of TiO_2 nanoparticles in such high pressure condition induces the growth of very thin TiO_2 nanowires, as reported by Wen et al., [56] that states the formation of ultra-long nanowires which may arise from the slow nucleation rate and very fast growth rate.

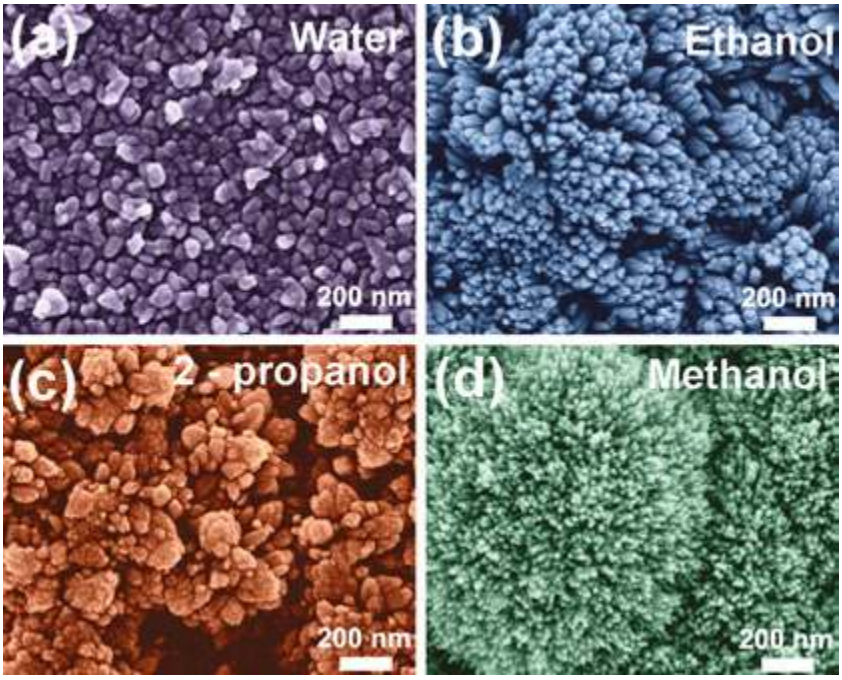

Figure 8. SEM images of TiO_2 nanostructures synthesized by solvothermal method, assisted by microwave radiation, using a microwave power of 100 W for 120 minutes and a temperature of 100°C for the solvents tested: (a) water, (b) ethanol, (c) 2 – propanol and (d) methanol. The insets show the cross-section of the produced TiO_2 nanostructures.

3.3. XRD analysis

Due to the intense XRD peak of PEN substrate at $2\theta = 26°$, GIXRD experiments were carried out for the TiO_2 nanostructures obtained with all the solvents tested. The results are presented on **Figure 9**, where it is possible to observe the experimental diffractograms for the different materials, together with the simulated diffractograms for anatase, rutile and brookite.

For all the materials synthesized, the XRD peaks could be assigned to either rutile or anatase. The nanorod arrays produced with water presented a predominant rutile phase, and the presence of anatase is not clear. This result is expected as the proportion of water/acid used during synthesis under microwave radiation has been reported to form essentially rutile [3]. For the materials synthesized with ethanol, as for the water arrays, just the rutile phase could

be assigned. The 2 – propanol solvent, on the other hand, can be expected to contain minor amounts of anatase, together with rutile. Methanol, just like the 2 – propanol arrays, is expected to have mainly the anatase phase and rutile. The appearance of the peak of PEN at ~48º is expected to be related to the thinner array thickness of the materials. Water formed thicker arrays, and the PEN peak is not evident.

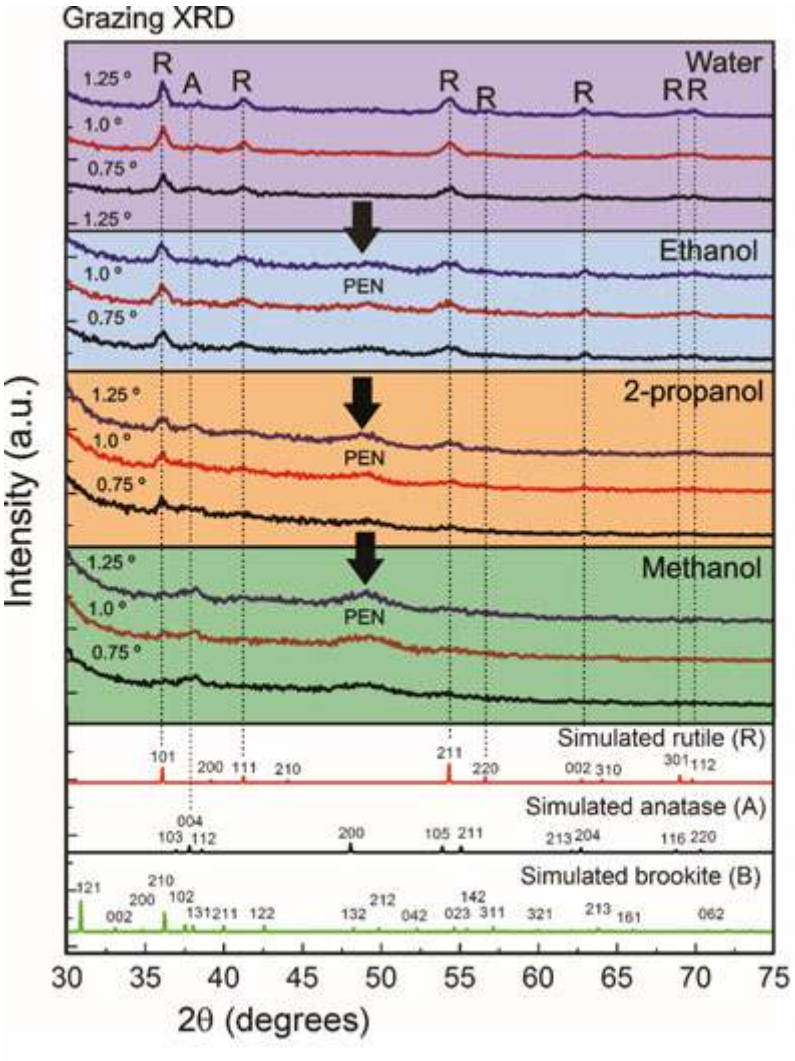

Figure 9. Grazing incident XRD diffractograms of TiO_2 nanostructured arrays produced with different solvents: water, ethanol, 2 – propanol and methanol. The grazing incident angles tested were 0.75, 1.0 and 1.25 °. The simulated rutile, anatase and brookite diffractograms are presented for comparison.

http://dx.doi.org/10.5772/63237

The coordination number of different types of alcohol can affect the final non-covalent bonding between molecules (oligomers) and the final structure of building blocks of a material. So, by using different types of solvents, it is possible to obtain a fivefold coordinated titanium and twofold coordinated oxygen in (1 0 1) plane of anatase phase of TiO_2 nanostructures instead of a fivefold coordinated titanium and two and threefold coordinated oxygen in (1 0 0) plane of rutile phase [5].

As reported by Yoon et al., [57], the TiO_2 crystal structure of the as-synthesized nanostructures, may change from anatase to rutile or brookite, with the number of carbon atoms to the solvent used for synthesis. The reaction between the precursor and the alcohol solvents become less vigorous with the increase in the number of carbon atoms.

3.4. Optical characterization

The bandgap of the TiO_2 nanostructured arrays were estimated from transmittance data through Tauc plots. Transmittance studies were carried out for the TiO_2 nanostructures produced with the different solvents tested. The optical bandgap (E_g) on the semiconductor is related to the optical transmittance coefficient (α) and the incident photon energy [58]. The relation can be given as:

$$\alpha(h\nu) = A(h\nu - E_g)^n$$

where α is the linear absorption coefficient of the material, $h\nu$ is the photon energy impinging on the material, A is a proportionality constant of the matrix density states and n is a constant exponent, that for the case of TiO_2 (a direct band gap semiconductor), presents the value, n = ½.

The following relation is obtained:

$$[\alpha(h\nu)]^2 = A(h\nu - E_g)$$

The bandgap can be estimated by plotting $[\alpha(h\nu)]^2$ against $h\nu$, and extracting the intersection of the extrapolation of the linear portion with zero in the photon energy axis, when no bandtails are considered [58]. The results are shown on **Figure 10**. Similar values were obtained for synthesis with water, ethanol and 2 – propanol, with a bandgap value of 3.2 eV. For methanol it was observed at a slight lower bandgap value of 3.16 eV. As most of the materials presented the rutile phase, and as the bandgap of a TiO_2 nanostructure is strongly dependent on the grain size and crystallographic phase, the presence of anatase (with a higher bandgap value) on TiO_2 nanostructured arrays could have influenced the bandgap values. Nevertheless, these values are within the values range reported in the literature for different crystallographic structures of TiO_2.

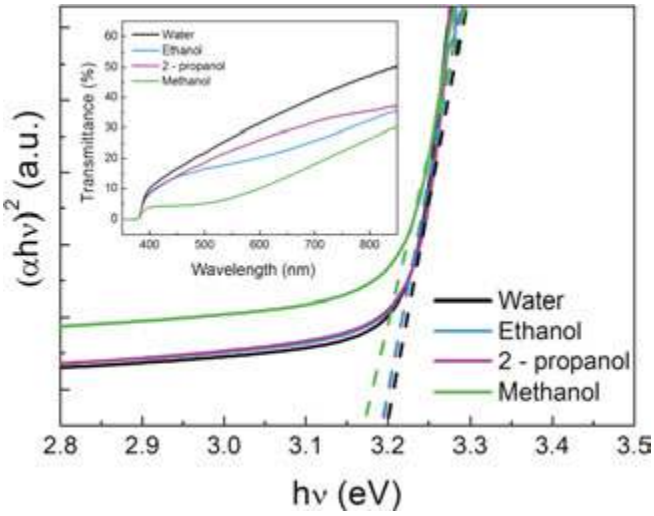

Figure 10. $[\alpha(h\nu)]^2$ variation versus photon energy hν. The inset shows the optical transmittance of TiO_2 nanostructured arrays on PEN substrate.

3.5. TiO_2 nanostructures arrays photocatalytic activity

Although it has been reported by several authors that the photocatalytic efficiency of anatase is higher than rutile or brookite, it has been recognized in the last few years that the simultaneous presence of all or some polymorphic phases may also be beneficial in photocatalytic applications [59].

The photocatalytic activity of TiO_2 nanostructures is related to the surface-phase structure and depends on different properties such as bandgap, crystallite size, specific surface are and active facets [60]. The TiO_2 active facets are {001} for anatase [22], {110} > {001} > {100} for rutile [11] and {210} for brookite [9].

The photocatalytic behaviour of different TiO_2 nanostructures arrays produced with the different solvents was evaluated by observing their efficiency on degrading the MB under UV radiation. **Figure 11** shows the photocatalytic results for the MB degradation with different TiO_2 nanostructures produced with each solvent tested. It is possible to observe that a gradual MB degradation occur under UV radiation, for all TiO_2 nanostructures produced, reaching values of 77% for water, 84% for ethanol, 79% for 2-propanol and 90% for methanol, after 120 min of exposure.

The higher MB degradation obtained for samples produced with methanol can be attributed to different factors, such as having a higher specific surface area (thin nanorods, relatively separated, when compared to the other morphologies) or by containing a greater amount of anatase as TiO_2 crystallographic phases, being directly related to the different exposed facets [3].

http://dx.doi.org/10.5772/63237

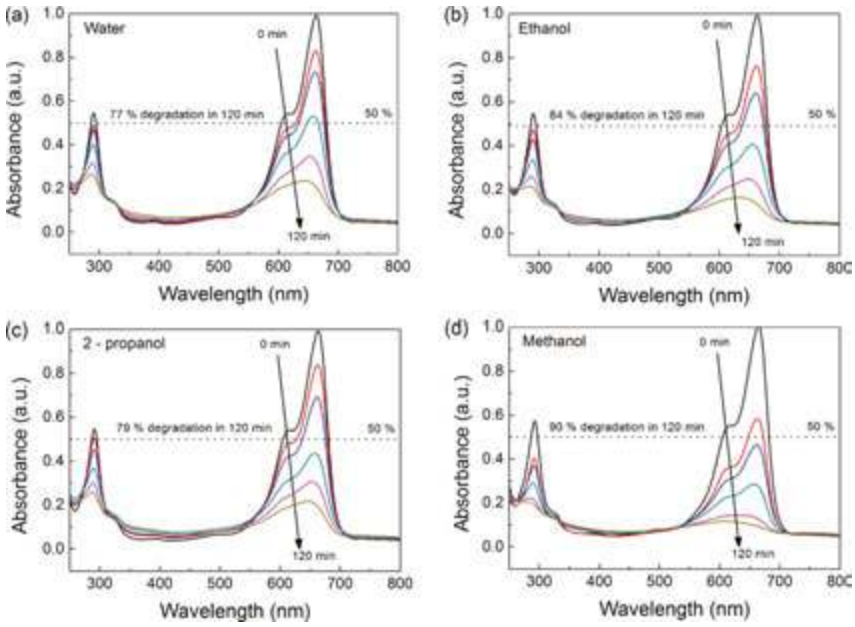

Figure 11. Normalized absorbance spectra of MB degradation under UV radiation as a function of exposure time in the presence of each TiO_2 nanostructured arrays synthesized with (a) water, (b) ethanol, (c) 2 - propanol and (d) methanol at room temperature and under an UV radiation of 160 nm, for 120 minutes.

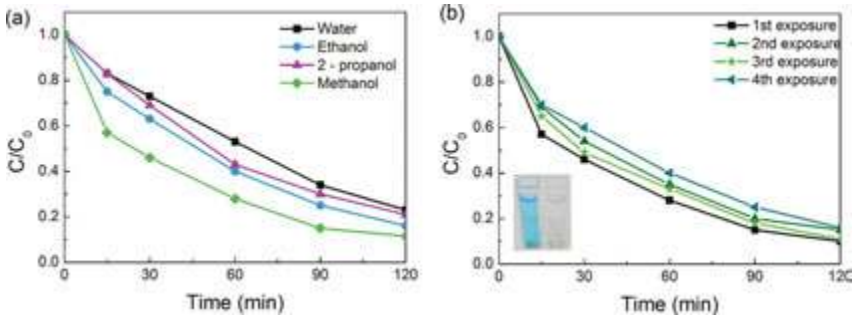

Figure 12. (a) MB concentration versus exposure time for the different photocatalysts produced with each solvent tested; (b) MB degradation ratio (C/C_0) *vs*. UV exposure time for the TiO_2 synthesized with methanol, after several UV exposure experiments. On the inset is possible to observe the colour difference in MB before and after the degradation experiment.

Figure 12.a presents the degradation ratio (C/C_0) as a function of UV exposure time, where C is the absorbance of the MB solution at each exposure time and C_0 is the absorbance of the initial solution [61]. By analyzing the obtained results, the methanol presents an initial higher efficiency on MB degradation; nevertheless for all the arrays produced, the MB degradation

appears to be continuous over time, with methanol always showing higher degradation for all UV exposure times. The efficiency of the TiO_2 nanostructured arrays synthesized with methanol under microwave radiation was confirmed and is presented in **Figure 12.b**. It is clear that the material presents remarkable stability and reusability after several UV exposures.

4. Conclusion

On the present chapter, we have shown the influence of using different solvents on the synthesis of TiO_2 nanostructured arrays under microwave radiation. The solvents played a crucial role on the final TiO_2 structure, which influenced directly their photocatalytic behaviour. Different TiO_2 nanostructures morphologies were obtained with an evident effect on the nanostructure sizes. The produced TiO_2 nanostructures arrays were essentially from rutile phase; nevertheless in some conditions they presented a mixture of crystallographic phases (rutile and anatase) which may enhance the photocatalytic activity of the nanostructured arrays. The optical bandgap of the materials were measured to be 3.16 and 3.2 eV, consistent with the theoretical values of the TiO_2 phases.

Regarding the photocatalytic degradation of methylene blue in the presence of TiO_2 nanostructured arrays, the ones synthesized with methanol presented a higher photocatalytic activity (90% over 120 min) probably due to its higher surface area, and taking the advantage of having higher amounts of the anatase phase. Some experiments were carried out to infer the stability and reproducibility for MB photodegradation with arrays synthesized with methanol, which demonstrated enhanced and comparable results after several exposure experiences.

Acknowledgements

This work has been financed by FEDER funds through the COMPETE 2020 programme and the Portuguese Science Foundation (FCT-MEC) through BPD/76992/2011 and BPD/84215/2012 and the Projects UID/CTM/50025/2013 and EXCL/CTM-NAN/0201/2012.

Author details

Ana Pimentel*, Daniela Nunes, Sónia Pereira, Rodrigo Martins and Elvira Fortunato*

*Address all correspondence to: acgp@campus.fct.unl.pt, emf@fct.unl.pt

CENIMAT/I3N, Department of Materials Science, Faculty of Science and Technology, NOVA University of Lisbon, FCT-UNL,Lisbon, Portugal

References

[1] Lee W.S., Park Y. S., Chou Y. K. Hierarchically Structured Suspended TiO_2 Nanofibers for Use in pH Sensor Devices. ACS Applied Materials Interfaces. 2014;6(12189–12195) DOI: http://dx.doi.org/10.1021/am501563v

[2] Roy P., Kim D., Lee K., Spiecker E., Schmuki P. TiO_2 nanotubes and their application in dye-sensitized solar cells. Nanoscale. 2010;2(45–49) DOI: 10.1039/b9nr00131j

[3] Nunes D., Pimentel A., Pinto J. V., Calmeiro T. R., Nandy S., Barquinha P., et al. Photocatalytic behavior of TiO_2 films synthesized by microwave irradiation. Catalysis Today. 2015; DOI: 10.1016/j.cattod.2015.10.038

[4] Ohno T., Lee S. Y., Yang Y. Fabrication of morphology-controlled TiO_2 photocatalyst nanoparticles and improvement of photocatalytic activities by modification of Fe compounds. Rare Metals. 2015;34(291–300) DOI: 10.1007/s12598-015-0483-8

[5] Golobostanfard M. R., Abdizadeh H. Effect of mixed solvent on structural, morphological, and optoelectrical properties of spin-coated TiO_2 thin films. Ceramics International. 2012;38(5843–5851) DOI: 10.1016/j.ceramint.2012.04.034

[6] Zhao L., Xia M., Liu Y., Zheng B., Jiang Q., Lian J. Structure and photocatalysis of TiO_2/ZnO double-layer film prepared by pulsed laser deposition. Materials Transactions. 2012;53(463–468) DOI: 10.2320/matertrans.M2011345

[7] Nakata K., Fujishima A. TiO_2 photocatalysis: Design and applications. Journal of Photochemistry and Photobiology C: Photochemistry Reviews. 2012;13(169–189) DOI: 10.1016/j.jphotochemrev.2012.06.001

[8] Lin H., Huang C., Li W. Ni C. Shah S., Tseng Y. Size dependency of nanocrystalline TiO_2 on its optical property and photocatalytic reactivity exemplified by 2-chlorophenol. Applied Catalysis B: Environmental. 2006;68(1–11) DOI: 10.1016/j.apcatb.2006.07.018

[9] Di Paola A., Bellardita M., Palmisano L. Brookite, the Least Known TiO_2 Photocatalyst. Catalysts. 2013;3(36–73) DOI: 10.3390/catal3010036

[10] Landmann M., Rauls E., Schmidt, W. G. The electronic structure and optical response of rutile, anatase and brookite TiO_2. Journal of physics. Condensed matter: an Institute of Physics journal. 2012;24(195503) DOI: 10.1088/0953-8984/24/19/195503

[11] Fujishima A., Rao T. N. Tryk D. A. Titanium dioxide photocatalysis. Journal of Photochemistry and Photobiology C: Photochemistry Reviews. 2000;1(1-21) DOI: 10.1016/S1389-5567(00)00002-2

[12] Sun W., Liu H., Hu J., Li,J. Controllable synthesis and morphology-dependent photocatalytic performance of anatase TiO_2 nanoplates. RSC Advances. 2015;5(513-520) DOI: 10.1039/C4RA13596B

[13] Tang H., Prasad K., Sanjinès R., Schmid P. E., Lévy F. Electrical and optical properties of TiO_2 anatase thin films. Journal of Applied Physics. 1994;75(2042) DOI: 10.1063/1.356306

[14] Daude N., Gout C., Jouanin C. Electronic band structure of titanium dioxide. Physical Review B. 1977;15(3229-3235) DOI: 10.1103/PhysRevB.15.3229

[15] Agrios A. G., Pichat P. State of the art and perspectives on materials and applications of photocatalysis over TiO_2. Journal of Applied Electrochemistry. 2005;35(7-8):(655-663) DOI: 10.1007/s10800-005-1627-6

[16] Li L., Salvador P. A., Rohrer G. S. Photocatalysts with internal electric fields. Nanoscale. 2014;6(1):(24-42) DOI: 10.1039/c3nr03998f

[17] Xu H., Ouyang S., Liu L., Reunchan P., Umezawa N., Ye J. Recent advances in TiO_2-based photocatalysis. Journal of Materials Chemistry A. 2014;2(32):(12642). DOI: 10.1039/C4TA00941J

[18] Pan L., Zou J. J., Wang S., Liu X. Y., Zhang X., Wang L. Morphology evolution of TiO_2 facets and vital influences on photocatalytic activity. ACS applied materials & interfaces. 2012;4(3):(1650-1655) DOI: 10.1021/am201800j

[19] Li J., Xu D. Tetragonal faceted-nanorods of anatase TiO_2 single crystals with a large percentage of active {100} facets. Chemical communications (Cambridge, England). 2010;46(13):(2301-2303) DOI: 10.1039/b923755k

[20] Kobayashi M., Kato H., Kakihana M. Synthesis of Titanium Dioxide Nanocrystals with Controlled Crystal- and Micro-structures from Titanium Complexes. Nanomaterials and Nanotechnology. 2013;3(1-10) DOI: 10.5772/57533

[21] Ohno T., Sarukawa K., Matsumura M. Crystal faces of rutile and anatase TiO_2 particles and their roles in photocatalytic reactions. New Journal of Chemistry. 2002;26(9): 1167-1170. DOI: 10.1039/b202140d

[22] Dozzi M., Selli E. Specific facets-dominated anatase TiO_2: fluorine-mediated synthesis and photoactivity. Catalysts. 2013;3(2):455-485. DOI: 10.3390/catal3020455

[23] Wang S., Qian H., Hu Y., Dai W., Zhong Y., Chen J., et al . Facile one-pot synthesis of uniform TiO_2–Ag hybrid hollow spheres with enhanced photocatalytic activity. Dalton Trans. 2013;42(4):1122-1128. DOI: 10.1039/C2DT32040A

[24] Sodano H. A., Koka A., Guskey C. R., Michael Seigler T., Bailey S. C. C. Introducing perturbations into turbulent wall-bounded flow with arrays of long TiO_2 nanowires. Journal of Fluids Engineering. 2014;137(2):024501. DOI: 10.1115/1.4027432

[25] Bauer S., Park J., Faltenbacher J., Berger S., von der Mark K., Schmuki P. Size selective behavior of mesenchymal stem cells on ZrO(2) and TiO(2) nanotube arrays. Integrative biology: quantitative biosciences from nano to macro. 2009;1(8-9):525-32. DOI: 10.1039/b908196h

[26] Lui G., Liao J.-Y., Duan A., Zhang Z., Fowler M., Yu A. Graphene-wrapped hierarchical TiO_2 nanoflower composites with enhanced photocatalytic performance. Journal of Materials Chemistry A. 2013;1(30):12255. DOI: 10.1039/c3ta12329d

[27] Lee J.-C., Park K.-S., Kim T.-G., Choi H.-J., Sung Y.-M. Controlled growth of high-quality TiO_2 nanowires on sapphire and silica. Nanotechnology. 2006;17(17):4317-4321. DOI: 10.1088/0957-4484/17/17/006

[28] Paulose M., Shankar K., Yoriya S., Prakasam H. E., Varghese O. K., Mor G. K., et al. Anodic growth of highly ordered TiO_2 nanotube arrays to 134 microm in length. The journal of physical chemistry. B. 2006;110(33):16179-84. DOI: 10.1021/jp064020k

[29] Song M. Y., Kim D. K., Ihn K. J., Jo S. M., Kim D. Y. Electrospun TiO_2 electrodes for dye-sensitized solar cells. Nanotechnology. 2004;15(12):1861-1865. DOI: 10.1088/0957-4484/15/12/030

[30] Kim S.-J., Lee E. G., Park S. D., Jeon C. J., Cho Y. H., Rhee C. K., et al. Hotocatalytic effects of rutile phase tio2 ultrafine powder with high specific surface area obtained by a homogeneous precipitation process at low temperatures. Journal of Sol-Gel Science and Technology. 2001;22(1-2):63-74. DOI: 10.1023/A:1011264320138

[31] Liu B., Aydil E. S. Growth of oriented single-crystalline rutile TiO(2) nanorods on transparent conducting substrates for dye-sensitized solar cells. Journal of the American Chemical Society. 2009;131(11):3985-90. DOI: 10.1021/ja8078972

[32] Nunes D., Pimentel A., Barquinha P., Carvalho,P. A., Fortunato E., Martins R. Cu_2O polyhedral nanowires produced by microwave irradiation. Journal of Materials Chemistry C. 2014;2(30):6097. DOI: 10.1039/C4TC00747F

[33] Pimentel A., Rodrigues J., Duarte P., Nunes D., Costa F. M., Monteiro T., et al. Effect of solvents on ZnO nanostructures synthesized by solvothermal method assisted by microwave radiation: a photocatalytic study. Journal of Materials Science2015. 2015;50(17):5777-5787. DOI: 10.1007/s10853-015-9125-7

[34] Pimentel A., Nunes D., Duarte P., Rodrigues J., Costa F. M., Monteiro T., et al. Synthesis of long ZnO nanorods under microwave irradiation or conventional heating. The Journal of Physical Chemistry C. 2014;118(26):14629-14639. DOI: 10.1021/jp5027509

[35] Gonçalves A., Resende J., Marques A. C., Pinto J. V., Nunes D., Marie A., et al. Smart optically active VO_2 nanostructured layers applied in roof-type ceramic tiles for energy efficiency. Solar Energy Materials and Solar Cells. 2015;150:1-9. DOI: 10.1016/j.solmat.2016.02.001

[36] Marques A. C., Santos L., Costa M. N., Dantas J. M., Duarte P., Gonçalves A., et al. Office paper platform for bioelectrochromic detection of electrochemically active bacteria using tungsten trioxide nanoprobes. Scientific reports. 2015;5:9910. DOI: 10.1038/srep09910

[37] Hays B. L. Microwave Synthesis: Chemistry at the Speed of Light. 1st ed. Michigan University: CEM Publishing; 2002. 295 p. DOI: ISBN-0-9722229-0-1

[38] Veggi, P., Martinez J., Meireles A. Microwave-assisted extraction for bioactive compounds. In: Chemat F., Cravotto G., editors. Food Engineering Series. 1st ed. Boston: Springer US; 2013. p. 15–52. DOI: 10.1007/978-1-4614-4830-3

[39] Lidström P., Tierney J., Wathey B., Westman J. Microwave assisted organic synthesis—a review. Tetrahedron. 2001;57(45):9225-9283. DOI: 10.1016/S0040-4020(01)00906-1

[40] Thostenson E. T., Chou T.-W. Microwave processing: fundamentals and applications. Composites Part A: Applied Science and Manufacturing. 1999;30(9):1055-1071. DOI: 10.1016/S1359-835X(99)00020-2

[41] Gabriel C., Gabriel S., Grant E. H., Halstead S.J., Mingos B.M.D. Dielectric parameters relevant to microwave dielectric heating. Chemical Society Reviews. 1998;27(3):213. DOI: 10.1039/a827213z

[42] Nemmaniwar B. G., Kalyankar N. V., Kadam P. L. Dielectric behaviour of binary mixture of 2-chloroaniline with 2-methoxyethanol and 2-ethoxyethanol. Orbital - The Electronic Journal of Chemistry. 2013;5(1):1-6. DOI: ISSN 1984-6428

[43] Kappe C. O. How to measure reaction temperature in microwave-heated transformations. Chemical Society reviews. 2013;42(12):4977-90. DOI: 10.1039/c3cs00010a

[44] Karpovich N. F., Pugachevskii M. A., Shtarev D. S. Influence of synthesis conditions on the shape and size characteristics of TiO_2 nanocrystals. Nanotechnologies in Russia. 2013;8(11-12):751-755. DOI: 10.1134/S1995078013060086

[45] Wu Z., Gu Z., Zhao W. Wang H. Photocatalytic oxidation of gaseous benzene over nanosized TiO_2 prepared by solvothermal method. Chinese Science Bulletin. 2007;52(22):3061-3067. DOI: 10.1007/s11434-007-0456-x

[46] Zhou, Y., Wu H., Zhong X., Liu C. Effects of non-polar solvent on the morphology and property of three-dimensional hierarchical TiO_2 nanostructures by one-step solvothermal route. Journal of Nanoparticle Research. 2014;16(7):2466. DOI: 10.1007/s11051-014-2466-3

[47] Wu Y.-C., Tai Y.-C. Effects of alcohol solvents on anatase TiO_2 nanocrystals prepared by microwave-assisted solvothermal method. Journal of Nanoparticle Research. 2013;15(6):1686. DOI: 10.1007/s11051-013-1686-2

[48] Kraus W., Nolzeb G. POWDER CELL – a program for the representation and manipulation of crystal structures and calculation of the resulting X-ray powder patterns. Journal of Applied Crystallography. 1996;29(3):301-303. DOI: 10.1107/S0021889895014920

[49] Pearson W. B., Villars P., Calvert L. D. Pearson's Handbook of CrystallographicData for Intermetallic Phases. 1st ed. Ohio, USA: ASM International; 1985. 2886 p. DOI: ISBN 10: 0871702177

[50] Saxena V. K., Chandra U. Microwave synthasis: a physical concept. In: Chandra U., editors. Microwave Heating. 1st ed. India: InTech; 2011. p. 3-22. DOI: 10.5772/22888

[51] Bilecka I., Niederberger M. Microwave chemistry for inorganic nanomaterials synthesis. Nanoscale. 2010;2(8):1358. DOI: 10.1039/b9nr00377k

[52] Wu Z., Yang S., Wu W. Shape control of inorganic nanoparticles from solution. Nanoscale. 2016;8(3):1237-59. DOI: 10.1039/c5nr07681a

[53] Polsongkram D., Chamninok P., Pukird S., Chow L., Lupan O., Cha, G., et al. Effect of synthesis conditions on the growth of ZnO nanorods via hydrothermal method. Physica B: Condensed Matter. 2008;403(19-20):3713-3717. DOI: 10.1016/j.physb. 2008.06.020

[54] Cao G. Nanostructures & Nanomaterials: Synthesis, Properties & Applications. 1st ed. London: Imperial College Press; 2004. 433 p. DOI: 1860944809

[55] Hu Z., Oskam G., Searson P. C. Influence of solvent on the growth of ZnO nanoparticles. Journal of Colloid and Interface Science. 2003;263(2):454-460. DOI: 10.1016/ S0021-9797(03)00205-4

[56] Wen B.-M., Liu C.-Y., Liu Y. Solvothermal synthesis of ultralong single-crystalline TiO_2 nanowires. New Journal of Chemistry. 2005;29(7):969. DOI: 10.1039/b502604k

[57] Yoon S., Lee E.-S., Manthiram A. Microwave-solvothermal synthesis of various polymorphs of nanostructured TiO_2 in different alcohol media and their lithium ion storage properties. Inorganic chemistry. 2012;51(6):3505-12. DOI: 10.1021/ic202239n

[58] Pankove J.I. Optical Processes in Semiconductors. 1st ed. New Jersey: Dover Publications, Inc.; 1971. 422 p. DOI: 0486602753

[59] Zeng H. C. Preparation and integration of nanostructured titanium dioxide. Current Opinion in Chemical Engineering. 2011;1(1):11-17. DOI: 10.1016/j.coche.2011.07.002

[60] Guo Y., Li H., Chen J., Wu X., Zhou L. TiO_2 mesocrystals built of nanocrystals with exposed {001} facets: facile synthesis and superior photocatalytic ability. J. Mater. Chem. A. 2014;2(46):19589-19593. DOI: 10.1039/C4TA05068A

[61] Zhou N., Polavarapu L., Gao N., Pan Y., Yuan P., Wang Q., et al. TiO_2 coated Au/Ag nanorods with enhanced photocatalytic activity under visible light irradiation. Nanoscale. 2013;5(10):4236-41. DOI: 10.1039/c3nr00517h